

## Experimental study on identification of stiffness change in a concrete frame experiencing damage and retrofit

X. T. Zhou<sup>†</sup>, J. M. Ko<sup>‡</sup> and Y. Q. Ni<sup>‡†</sup>

*Department of Civil and Structural Engineering, The Hong Kong Polytechnic University,  
Hung Hom, Kowloon, Hong Kong*

*(Received November 3, 2005, Accepted August 11, 2006)*

**Abstract.** This paper describes an experimental study on structural health monitoring of a 1:3-scaled one-story concrete frame subjected to seismic damage and retrofit. The structure is tested on a shaking table by exerting successively enhanced earthquake excitations until severe damage, and then retrofitted using fiber-reinforced polymers (FRP). The modal properties of the tested structure at trifling, moderate, severe damage and strengthening stages are measured by subjecting it to a small-amplitude white-noise excitation after each earthquake attack. Making use of the measured global modal frequencies and a validated finite element model of the tested structure, a neural network method is developed to quantitatively identify the stiffness reduction due to damage and the stiffness enhancement due to strengthening. The identification results are compared with 'true' damage severities that are defined and determined based on visual inspection and local impact testing. It is shown that by the use of FRP retrofit, the stiffness of the severely damaged structure can be recovered to the level as in the trifling damage stage.

**Keywords:** concrete frame; shaking table test; seismic damage; retrofit; structural stiffness identification; neural network.

---

### 1. Introduction

Civil structures suffer from damage over their service life due to attacks from natural hazards such as earthquakes, fires, hurricanes, long-term fatigue and corrosion. For critical structures such as hospitals, power stations, major bridges, it is imperative that their health be assessed immediately after a major hazardous event. Knowledge of damage is the basis for decision making on whether retrofitting, partial replacement or demolition is necessary after severe hazards. Recent natural hazards such as Niigata Earthquake in Japan in 2004 and Kashmir Earthquake in Pakistan in 2005 have highlighted the need for real-time damage assessment of civil structures with widespread societal implications. From the perspective of both structural safety and serviceability, the detection of structural damage is the starting point for enhanced performance of buildings and bridges after long-term usage.

---

<sup>†</sup> PhD

<sup>‡</sup> Chair Professor, E-mail: [cejmko@inet.polyu.edu.hk](mailto:cejmko@inet.polyu.edu.hk)

<sup>‡†</sup> Associate Professor, Corresponding author, E-mail: [ceyqni@polyu.edu.hk](mailto:ceyqni@polyu.edu.hk)

Assessing damage to building structures during earthquakes has been widely studied by defining various damage indices (Park and Ang 1985, Stephens and Yao 1987, DiPasquale *et al.* 1990, Cabanas *et al.* 1997, Ghobarah *et al.* 1999, Cosenza and Manfredi 2000, Elenas and Meskouris 2001). These investigations were focused on overall structural damage evaluation by means of nonlinear seismic response analysis without directly using measurement data. With the advances in sensor and computer technologies, increasing research interests have been given on damage identification by the use of measurement data of structural dynamic response and modal properties (Hassiotis and Jeong 1995, Koh *et al.* 1995, Skjærbaek *et al.* 1998, Escobar *et al.* 2001, Huang *et al.* 2003, Ge and Lui 2005). The premise underlying the vibration-based damage identification approach is that structural damage in terms of stiffness reduction will result in change of modal properties (natural frequencies, modal shapes and modal damping). By detecting the change in measured modal parameters, the element-level damage of a structure can be assessed by applying a system identification algorithm. Among system identification algorithms available, neural network technique, because of its powerful learning capacity and high tolerance to incomplete and partially inaccurate data, has been shown promising for structural damage detection (Wu *et al.* 1992, Elkordy *et al.* 1994, Zhao *et al.* 1998, Kim *et al.* 2000, Yun *et al.* 2001, Ni *et al.* 2002).

This paper presents an experimental investigation of identifying stiffness change in a concrete frame due to seismic damage and post-earthquake retrofit by using a neural network approach. A 1:3-scaled one-story concrete frame was tested on a shaking table by exerting successively enhanced earthquake excitations to generate trifling, moderate, and severe damage, respectively, and then retrofitted using the fiber-reinforced polymer (FRP) technique. After experiencing the earthquake excitations at each level, the structure was subjected to a white-noise random excitation of low intensity at its base to generate ambient vibration, and the excitation and response during the ambient vibration were measured for modal parameter identification. Free vibration tests were also conducted. A back-propagation (BP) neural network with appropriate configuration is trained using simulated data from a validated finite element model, and then the measured modal frequencies are fed into the trained neural network to identify the stiffness change in each structural member caused by seismic damage and retrofit. Because the true damage severities are unknown for the tested structure, separate impact testing has been conducted on individual structural members at each damage/strengthening stage, from which the member local modal parameters were obtained and used to assess the 'real' damage extent for comparison with the identified results by the neural network approach making use of global modal data.

## 2. Shaking table tests

A one-story concrete frame shown in Fig. 1, which is 1:3 scaled down from a real structure, is fabricated for shaking table tests. It is 2.3 m long, 1.4 m wide and 1.9 m high. The two columns in the frame have the same cross section of 100 mm by 100 mm, and the three walls have the same cross section of 300 mm by 50 mm. The thickness of the upper and bottom slabs is 150 mm. The central wall is perpendicular to other two walls on one side. The bottom slab of the tested structure is fixed on the shaking table, and the upper slab is supported by the two columns and the three walls. A 0.75-ton mass block is laid on each corner of the upper slab to simulate the load transformed from upper floor in the prototype structure. Fig. 2 shows the arrangement of reinforcement for the column cross-section (only longitudinal reinforcement has been considered



Fig. 1 Tested frame

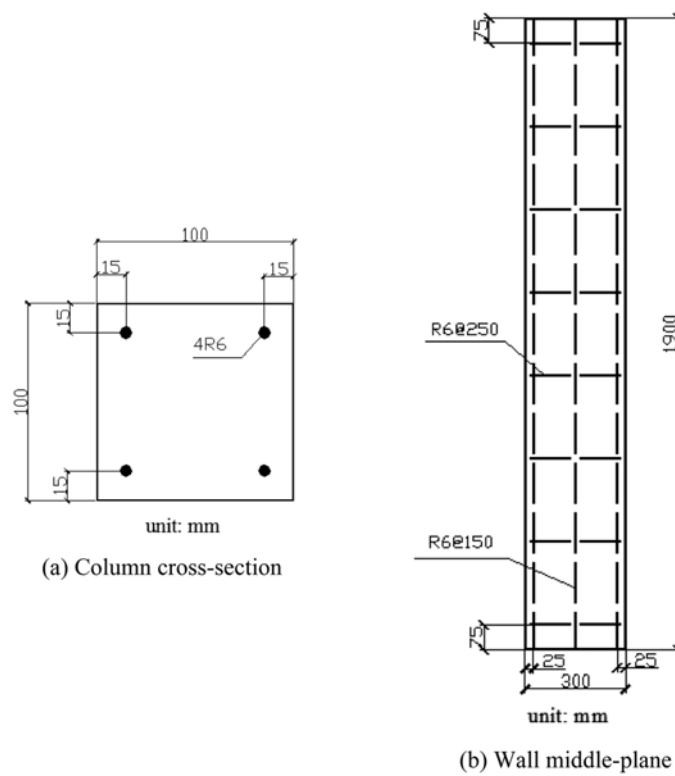


Fig. 2 Arrangement of reinforcement for columns and walls

because of the limited cross-section size) and for the wall middle-plane. There is no reinforcement for the upper and bottom slabs. The percentage of total longitudinal reinforcement satisfies the requirement prescribed in the Hong Kong design code (Buildings Department 2004). The concrete grade is C35.

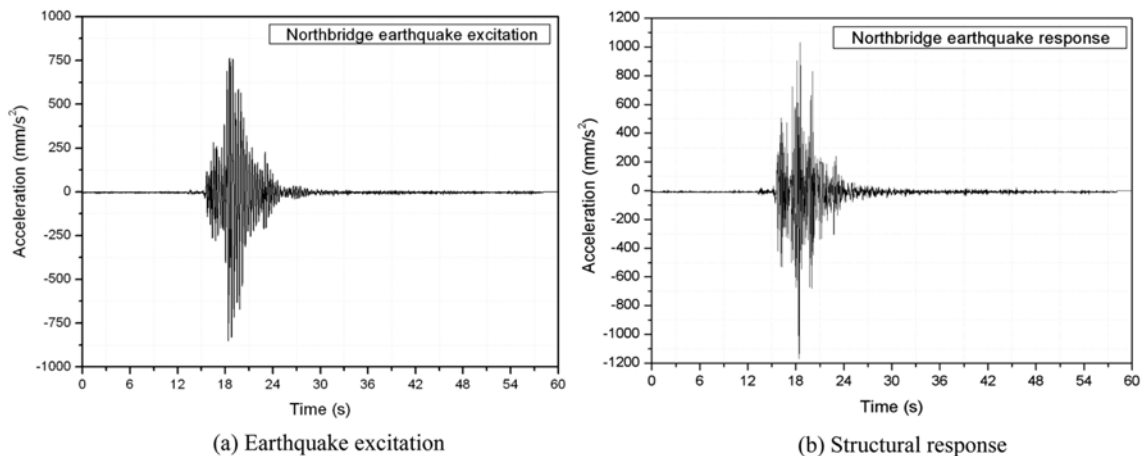


(a) Trifling damage in wall

(b) Moderate damage in wall

(c) Severe damage in wall

Fig. 3 Visual inspection of damage after three levels of earthquake excitations



(a) Earthquake excitation

(b) Structural response

Fig. 4 Time history of earthquake excitation and structural response

The structure was tested on a 3 m by 3 m shaking table with successively enhanced earthquake excitations (modulated Northbridge Earthquake with increasing magnitude). Accordingly, the structure incurred trifling, moderate and severe damage respectively at different test stages. The seismic damage mainly manifests itself as cracks in the columns and the walls and at connections between the slabs and the columns and between the slabs and the walls as shown in Fig. 3. The number and size of the cracks increase with the increase of earthquake intensity. According to a roughly estimated relationship between the damage severity (in terms of observed size and number of cracks) and the peak value of the earthquake acceleration excitation, three levels of earthquake excitation and damage extent are defined: the trifling damage corresponds to the earthquake excitations with peak acceleration from 0.05 to 0.20 g, the moderate damage corresponds to the earthquake excitations with peak acceleration from 0.20 to 0.40 g, and the severe damage corresponds to the earthquake excitations with peak acceleration from 0.40 to 0.90 g. Fig. 4 illustrates an exerted earthquake excitation and the corresponding response of the tested structure at the central point of the upper slab during the shaking table tests.

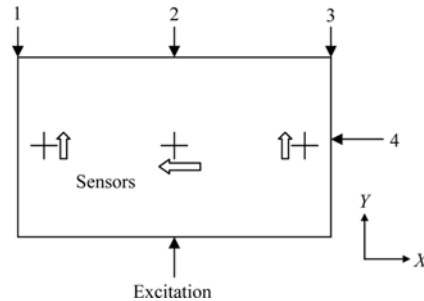


Fig. 5 Schematic of excitation and sensor locations

After experiencing each level of earthquake excitations, a visual inspection is carefully conducted on every column and wall to check the presence and evolution of cracks. Then an experimental modal test is carried out on the structure to acquire the global modal properties, followed by imposing a hammer impact on every structural member to obtain the local modal properties for the purpose of verification. As shown in Fig. 5, three accelerometers (denoted as ‘+’) are positioned at the bottom slab for excitation measurement while other three accelerometers (denoted by arrows) are deployed at the upper slab for response measurement. The oriented direction of the accelerometers at the upper slab is designated by the arrows in Fig. 5 (one in parallel to  $X$ -axis is in horizontal ‘ $\leftrightarrow$ ’ direction and two in parallel to  $Y$ -axis are in horizontal ‘ $\uparrow$ ’ direction), and the accelerometers at the bottom slab are oriented in the same direction as their counterparts at the upper slab. Moreover, when conducting local impact testing on a specific member (column and wall), an accelerometer is installed at the middle of the member to capture the local dynamic properties. In each modal test, the following procedure is complied with:

- i. The structure is subjected to small-amplitude (about 0.01 g) white-noise excitation with a frequency range of 1 Hz ~15 Hz by the shaking table;

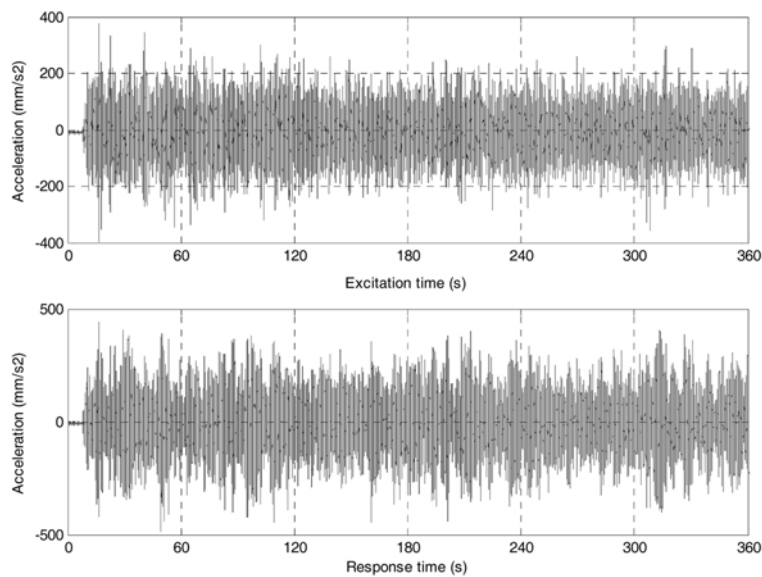


Fig. 6 White-noise random excitation and response

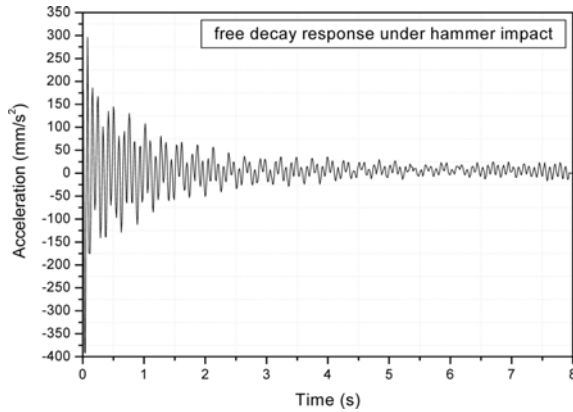


Fig. 7 Free vibration response under hammer impact



Fig. 8 FRP-retrofitted structure

Table 1 Description of damage/strengthening cases

Case	Health status	Location of new cracks
1	No damage	N/A
2	Trifling damage	C1 (T, M & B), C2 (M & B), W1 (T & B)
3	Moderate damage	C1 (B), C2 (T & B), W1 (T & B), W2 (T & B), W3 (T)
4	Severe damage	C1 (T), C2 (T), W1 (T, M & B), W2 (T & B), W3 (T & B)
5	Retrofit by FRP	All cracks repaired

- ii. The structure is subjected to hammer impacts at the locations 1, 2, 3 and 4 (refer to Fig. 5) of the upper slab respectively to produce global free vibration;
- iii. A hammer impact is imposed transversely on the center of each column and wall in turn to excite member local vibration.

Fig. 6 illustrates the white-noise excitation and the response at the central point of the upper slab after the structure incurred trifling damage. Fig. 7 shows the free vibration response of the structure at the same point when a hammer impact is acted on the location 2. The above test procedure is repeated to obtain the global and local dynamic properties of the structure at trifling, moderate and severe damage stages. After suffering from severe damage, the structure is retrofitted using FRP as shown in Fig. 8, and then the above test procedure is conducted again.

The five test stages and the corresponding visual inspection results of structural health status are summarized in Table 1, where N/A denotes no damage; C1, C2, W1, W2, and W3 denote column 1, column 2, wall 1, wall 2, and wall 3, respectively; T, M, and B denote the top, middle and bottom portions of a column or wall, respectively.

### 3. Processing of measurement data

The global modal properties of the tested structure at the five stages are identified from: (i) spectral analysis using only the measured acceleration responses under white-noise excitation which simulate the post-earthquake ambient vibration measurement, (ii) frequency response functions

Table 2 Measured global modal frequencies

Case	Frequency (Hz)		
	1st	2nd	3rd
1	4.692	7.625	12.904
2	3.910	5.865	11.730
3	2.447	4.895	10.769
4	1.951	4.877	6.828
5	3.901	5.852	8.778

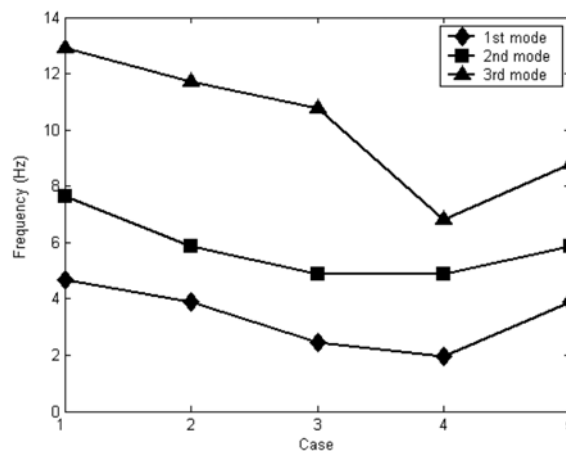


Fig. 9 Measured frequencies versus damage/strengthening case

obtained using both the white-noise excitation and response measurements, and (iii) free decay vibration responses obtained by hammer impact, respectively. It is found that the identified modal frequencies obtained by the three approaches are identical, whereas the modal vectors (mode shapes) and damping ratios identified from different approaches are highly inconsistent. It is therefore decided to use only the measured modal frequencies for damage diagnosis. The modal identification results show that the first global mode is a torsional mode, and the second and third global modes correspond to translational motions in the two horizontal directions respectively. The measured frequencies of the first three global modes are summarized in Table 2 and their variation with successive damage and strengthening is illustrated in Fig. 9.

The above measured global modal frequencies will be used to identify the change of structural stiffness caused by seismic damage and retrofit by means of a neural network approach. Although a careful visual inspection on the cracks has been made at each stage, quantification of the real damage is not available. In order to verify the identification results, local impact testing has been conducted on each column and wall in turn to obtain the local vibration frequency of individual structural members. With the measured local frequency, we can evaluate the member stiffness loss by regarding each member (column or wall) as a beam with fixed ends, and then presume it as nominal ‘real’ damage for verification of the global identification results. The  $r$ th bending frequency of a beam can be expressed as

Table 3 Identified local frequency and member stiffness loss

Case	Local frequency (Hz) and percentage stiffness loss (%)									
	Column 1		Column 2		Wall 1		Wall 2		Wall 3	
	$f_{C1}$	$\Delta k_{C1}$	$f_{C2}$	$\Delta k_{C2}$	$f_{W1}$	$\Delta k_{W1}$	$f_{W2}$	$\Delta k_{W2}$	$f_{W3}$	$\Delta k_{W3}$
1	147.3	0.00	154.1	0.00	87.8	0.00	220.6	0.00	242.3	0.00
2	124.2	28.94	133.9	24.51	64.5	46.01	189.5	26.21	206.5	27.38
3	96.5	57.07	99.4	58.40	59.2	54.47	124.6	68.12	132.0	70.32
4	88.8	63.68	82.0	71.69	48.8	69.13	103.2	78.13	106.8	80.56
5	123.9	29.26	124.8	34.37	78.0	20.99	193.3	23.25	207.2	26.86

$$f_r = \frac{(\beta_r L)^2}{2\pi} \sqrt{\frac{EI}{mL^4}} \quad (1)$$

where  $\beta_r$  is a coefficient relevant to boundary condition and mode order;  $L$ ,  $m$  and  $EI$  are length, mass density and bending stiffness of the member, respectively. Assuming that the length, mass and boundary condition remain the same before and after damage, it is known from Eq. (1) that the reduction of the bending stiffness is proportional to the difference of  $f_r^2$ , and therefore can be estimated using the measured pre- and post-damage local frequency  $f_r$ . The first bending frequency and the stiffness loss of each structural member evaluated from the local impact testing are summarized in Table 3.

#### 4. Finite element modeling

A neural network approach will be explored to identify the structural damage from the measured global frequencies before and after damage. A three-dimensional finite element model (FEM) of the tested structure is developed by means of the commercial software package ABAQUS to produce analytical data for the training of a feed-forward neural network with back-propagation algorithm. The developed FEM involves 32 nodes and 27 elements, in which the upper and bottom slabs are modeled as rigid-body elements; each column or wall is modeled by three Timoshenko beam elements; and the four mass blocks at the corners of the upper slab are represented by mass elements. The Timoshenko beam elements take into consideration the flexural rigidity, shear rigidity and torsional rigidity in formulating the stiffness matrix; as a result, the effect of damage on the flexural, shear and torsional properties of structural members can be explicitly represented in the FEM.

Table 4 Comparison of measured and analytical frequencies

Mode	Measured results (Hz)	FEM results (Hz)	Relative difference (%)
1st	4.692	4.693	0.021
2nd	7.625	7.635	0.131
3rd	12.904	12.807	-0.752

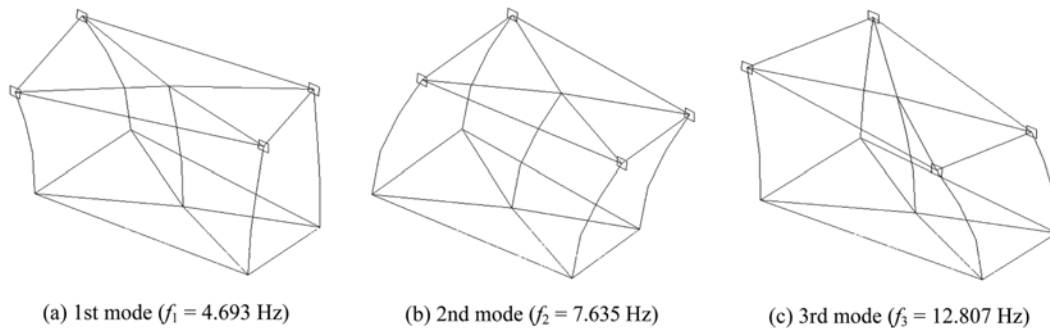


Fig. 10 Analytical mode shapes obtained by FEM

The FEM is calibrated and refined using the measured first three global modal frequencies of the intact structure (Case 1). The model refinement is accomplished by adjusting the Young's modulus to achieve the best fit between the measured and predicted frequencies. Table 4 shows a comparison of the measured and analytical frequencies for the first three modes after the model refinement. It is seen that the maximum relative difference is 0.752%, which is even lower than 1%. So the validated FEM captures the global modal properties of the tested structure well and is appropriate for damage simulation. The mode shapes were also calibrated by using the measured modal data. The first three analytical modes are evaluated to be a torsional mode and two bending modes along the horizontal axes respectively, identical with the measured mode shapes. Fig. 10 illustrates the analytically obtained mode shapes of the first three modes of the intact structure. With the validated FEM, we can simulate a series of damage scenarios analytically to produce training samples of the neural network.

## 5. Damage identification using neural network

With the measured global modal data and the developed FEM, a neural network is configured to perform the identification of damage extent at each stage. The neural network is used to map the relation between the modal properties (input) and the structural health status (output). The calculated modal parameters from the FEM with simulated damage scenarios are used to train the neural network, and the measured modal data for true damage scenarios will be fed into the trained neural network for damage identification.

### 5.1 Damage modeling and neural network configuration

As mentioned earlier, the seismic damage of the tested structure appears mainly as cracks in the structural members. While some researchers have addressed crack detection by formulating crack elements or indices in compliance with fracture mechanics concepts (Qian *et al.* 1990, Liang *et al.* 1992, Hjelmstad and Shin 1996, Morassi 2001, Kim and Stubbs 2003), the present study aims to evaluate the member stiffness change due to seismic damage and retrofit. It is therefore assumed that: (i) the cracks presented in a column or wall will lead to the loss of member bending and torsional stiffness regardless of crack locations; (ii) the stiffness loss can be expressed equivalently

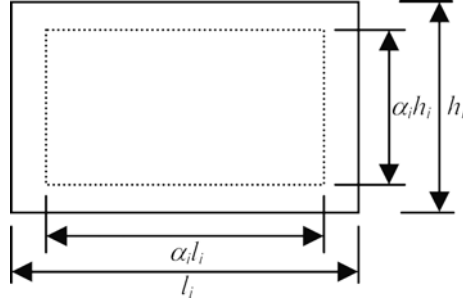


Fig. 11 Modeling of member damage

as a reduction in cross-sectional area of structural members along the member length; and (iii) the damage results in a proportional reduction of the two dimensions in cross section. Based on these assumptions, the damage modeling, as illustrated in Fig. 11, is described as

For the  $i$ th structural member (column or wall), the area of member cross section is defined as  $l_i \times h_i$ . After damage, the cross-sectional area is reduced to  $\alpha_i l_i \times \alpha_i h_i$ .

Because we assume that material properties remain unchanged after damage, stiffness reduction of the  $i$ th member caused by damage is only a function of the parameter  $\alpha_i$ . Consequently, the damage detection is intended to identify the value of  $\alpha_i$  at each stage.

A feed-forward neural network with back-propagation training algorithm is configured for damage identification. A total of five frequency-derived parameters  $DF_T$ ,  $DF_X$ ,  $DF_Y$ ,  $DF_X/DF_T$ , and  $DF_Y/DF_T$  are adopted to constitute the input vector, and therefore the network has five input nodes. Here  $DF_T$ ,  $DF_X$  and  $DF_Y$  are the change ratios of the torsional,  $X$ -direction bending and  $Y$ -direction bending global frequencies before and after damage, defined by

$$DF_i = \frac{F_i^d - F_i^u}{F_i^u} \quad (2)$$

where  $F_i^u$  and  $F_i^d$  are the global modal frequency of the structure before and after damage; the subscript  $i$  is taken as  $X$ ,  $Y$  and  $T$  which denotes  $X$ -direction bending mode,  $Y$ -direction bending mode and torsional mode, respectively. Although the reduction of stiffness is directly proportional to the difference of the square of modal frequencies before and after damage, here we use the relative difference of modal frequencies as input to the neural network because this parameter is more tolerant of modeling error than the difference of the square of modal frequencies when using FEM-generated modal frequencies as training samples.

Because only global modal frequencies exclusive of modal vectors are used for damage detection, it is difficult to distinguish between the two symmetrically located side columns and distinguish between the two symmetrically located side walls. So the five members are grouped into three sets: side columns (column 1 and column 2), central wall (wall 1), and side walls (wall 2 and wall 3). As a result, only three parameters,  $\alpha_1$ ,  $\alpha_2$  and  $\alpha_3$ , are issued as target output of the neural network to be identified.

The number of hidden layers and the number of hidden nodes are determined by trial and error. With the finite element model of the tested structure, damage scenarios present at various members are simulated to produce training samples which are used to train a set of neural networks with different hidden layers and hidden nodes. Then the trained neural networks are tested by feeding

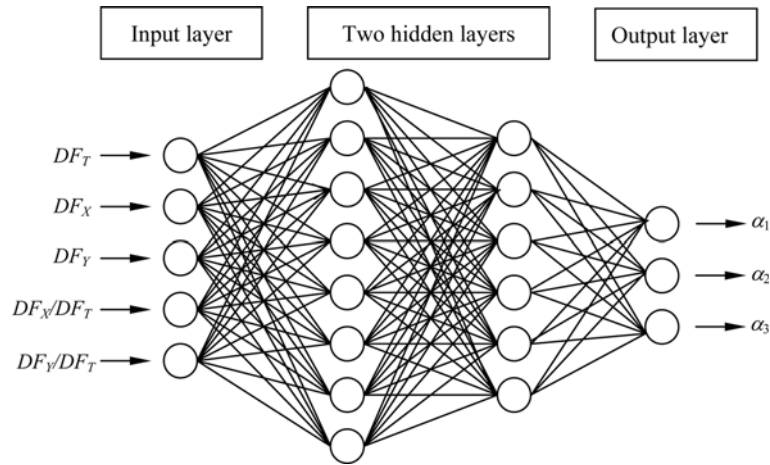


Fig. 12 Four-layer neural network configuration

them with simulated data from new damage scenarios, and the best hidden configuration is determined from the neural network which produces the most accurate identification for the simulated data. Fig. 12 shows the topology of such obtained neural network with the best configuration, which consists of two hidden layers with eight and six nodes each. Thus, a four-layer neural network with the configuration of 5-8-6-3 is constructed for damage identification with the use of measured global modal frequencies.

### 5.2 Neural network training and identification results

The configured four-layer neural network is trained by using back-propagation algorithm. The training samples are generated using analytical modal data from the validated finite element model by changing the values of  $\alpha_1$ ,  $\alpha_2$  and  $\alpha_3$ . To make the training samples as closely as possible with the true damage cases, the values of  $\alpha_1$ ,  $\alpha_2$  and  $\alpha_3$  are varied from 0.68 to 0.98 at an interval of 0.02 to generate training patterns. In addition, proper combinations of  $\alpha_1$ ,  $\alpha_2$  and  $\alpha_3$  are also considered to generate the training samples representing multi-damage cases. A total of 98 training samples have been generated to train the neural network.

Then the measured global modal frequencies at each stage (including the intact case and the strengthening case) are taken as the testing samples for damage identification. By presenting the measured frequencies at each stage into the trained neural network, the output indicates the identified stiffness reduction coefficients. Table 5 shows the identification results for all five cases. In this table the 'real' stiffness losses assessed by local impact testing are also provided for comparison. It should be noted that the global identification method can only indicate the average stiffness loss of columns 1 and 2 and walls 2 and 3. Even so, the identification results coincide fairly well with both the visual inspection results shown in Table 1 and the 'real' stiffness losses identified by local impact testing. More importantly, the identification results provide a quantitative evaluation of the stiffness enhancement after retrofit. From Table 5, it is seen that making use of FRP retrofit, the stiffness of the severely damaged structure is recovered to the level as in the trifling damage stage, indicating the effectiveness of strengthening by the FRP technique.

Table 5 Identification results

Case	Structural member	'Real' stiffness loss (%)	Identified stiffness loss (%)
1	Column 1	0.0	2.43
	Column 2	0.0	2.43
	Wall 1	0.0	0.59
	Wall 2	0.0	0.74
	Wall 3	0.0	0.74
2	Column 1	28.94	32.8
	Column 2	24.51	32.8
	Wall 1	46.01	39.9
	Wall 2	26.21	34.46
	Wall 3	27.38	34.46
3	Column 1	57.07	64.05
	Column 2	58.40	64.05
	Wall 1	54.47	52.90
	Wall 2	68.12	72.21
	Wall 3	70.32	72.21
4	Column 1	63.68	71.75
	Column 2	71.69	71.75
	Wall 1	69.13	65.02
	Wall 2	78.13	71.73
	Wall 3	80.56	71.73
5	Column 1	29.26	31.89
	Column 2	34.37	31.89
	Wall 1	20.99	41.90
	Wall 2	23.25	36.16
	Wall 3	26.86	36.16

## 6. Conclusions

This paper presents a shaking table experimental study on post-earthquake damage identification and structural retrofit assessment of a concrete frame structure. By modeling the structural damage and strengthening in terms of stiffness change, the health monitoring is issued to identify the equivalent stiffness reduction coefficients of structural members. The identification is conducted by using the measured global modal properties and an appropriately configured neural network. In this study, only the first three global modal frequencies are used for damage assessment. Because true damage severities are unknown for the tested structure, separate impact testing has also been conducted on individual structural members, from which the member local modal parameters are obtained and used to assess the 'real' damage for comparison with the identified results from the global testing. With the identification results, it is verified that the seismic damage occurs in both columns and walls and the damage extent increases gradually from case 1 to case 4. The proposed method also provides a feasible approach to quantitatively evaluating the effectiveness of structural

retrofit. The identification results indicate that the FRP retrofit recovers the stiffness of the severely damaged structure to the level as in the trifling damage stage.

## Acknowledgements

The work described in this paper was supported by a grant from The Hong Kong Polytechnic University (Project No. 87KP).

## References

- Buildings Department (2004), *Code of Practice for Structural Use of Concrete*, The Government of the Hong Kong Special Administrative Region, Hong Kong.
- Cabanas, L., Benito, B. and Herraiz, M. (1997), "An approach to the measurement of the potential structural damage of earthquake ground motions", *Earthq. Eng. Struct. Dyn.*, **26**, 79-92.
- Cosenza, E. and Manfredi, G. (2000), "Damage indices and damage measures", *Progress in Structural Engineering and Materials*, **2**, 50-59.
- DiPasquale, E., Ju, J.-W., Askar, A. and Cakmak, A.S. (1990), "Relation between global damage indices and local stiffness degradation", *J. Struct. Eng.*, ASCE, **116**, 1440-1456.
- Elenas, A. and Meskouris, K. (2001), "Correlation study between seismic acceleration parameters and damage indices of structures", *Eng. Struct.*, **23**, 698-704.
- Elkordy, M.F., Chang, K.C. and Lee, G.C. (1994), "A structural damage neural network monitoring system", *Microcomputers in Civil Engineering*, **9**, 83-96.
- Escobar, J.A., Sosa, J.J. and Gomez, R. (2001), "Damage detection in framed buildings", *Canadian J. Civil Eng.*, **28**, 35-47.
- Ge, M. and Lui, E.M. (2005), "Structural damage identification using system dynamic properties", *Comput. Struct.*, **83**, 2185-2196.
- Ghobarah, A., Abou-Elfath, H. and Biddah, A. (1999), "Response-based damage assessment of structures", *Earthq. Eng. Struct. Dyn.*, **28**, 79-104.
- Hassiotis, S. and Jeong, G.D. (1995), "Identification of stiffness reductions using natural frequencies", *J. Eng. Mech.*, ASCE, **121**, 1106-1113.
- Hjelmstad, K.D. and Shin, S. (1996), "Crack identification in a cantilever beam from modal response", *J. Sound Vib.*, **198**, 527-545.
- Huang, C.S., Hung, S.L., Wen, C.M. and Tu, T.T. (2003), "A neural network approach for structural identification and diagnosis of a building from seismic response data", *Earthq. Eng. Struct. Dyn.*, **32**, 187-206.
- Kim, J.-T. and Stubbs, N. (2003), "Nondestructive crack detection algorithm for full-scale bridges", *J. Struct. Eng.*, ASCE, **129**, 1358-1366.
- Kim, S.-H., Yoon, C. and Kim, B.-J. (2000), "Structural monitoring system based on sensitivity analysis and a neural network", *Computer-Aided Civil and Infrastructure Engineering*, **15**, 309-318.
- Koh, C.G., See, L.M. and Balendra, T. (1995), "Damage detection of buildings: Numerical and experimental studies", *J. Struct. Eng.*, ASCE, **121**, 1155-1160.
- Liang, R.Y., Hu, J. and Choy, F. (1992), "Theoretical study of crack-induced eigenfrequency changes on beam structures", *J. Eng. Mech.*, ASCE, **118**, 384-396.
- Morassi, A. (2001), "Identification of a crack in a rod based on changes in a pair of natural frequencies", *J. Sound Vib.*, **242**, 577-596.
- Ni, Y.Q., Wang, B.S. and Ko, J.M. (2002), "Constructing input vectors to neural networks for structural damage identification", *Smart Materials and Structures*, **11**, 825-833.
- Park, Y.J. and Ang, A.H.-S. (1985), "Mechanistic seismic damage model of reinforced concrete", *J. Struct. Eng.*, ASCE, **111**, 722-739.

- Qian, G.L., Gu S.N. and Jiang, J.S. (1990), "The dynamic behaviour and crack detection of a beam with a crack", *J. Sound Vib.*, **138**, 233-243.
- Skjærbæk, P.S., Nielsen, S.R.K., Kirkegaard, P.H. and Cakmak, A.S. (1998), "Damage localization and quantification of earthquake excited RC-frames", *Earthq. Eng. Struct. Dyn.*, **27**, 903-916.
- Stephens, J.E. and Yao, J.P.T. (1987), "Damage assessment using response measurements", *J. Struct. Eng.*, ASCE, **113**, 787-801.
- Wu, X., Ghaboussi, J. and Garrett, J.H., Jr. (1992), "Use of neural networks in detection of structural damage", *Comput. Struct.*, **42**, 649-659.
- Yun, C.-B., Yi, J.-H. and Bahng, E.Y. (2001), "Joint damage assessment of framed structures using neural networks technique", *Eng. Struct.*, **23**, 425-435.
- Zhao, J., Ivan, J.N. and DeWolf, J.T. (1998), "Structural damage detection using artificial neural networks", *Journal of Infrastructure Systems*, ASCE, **4**, 93-101.